Original Article

DOI: 10.5582/ddt.2016.01055

In vitro and *in vivo* biophysical properties of oligonucleotides containing 5'-thio nucleosides

Md Ariful Islam[1,*], Reiko Waki[1,*], Aki Fujisaka[1,2,*], Kosuke Ramon Ito[1], Satoshi Obika[1,]**

[1] *Graduate School of Pharmaceutical Sciences, Osaka University, Osaka, Japan;*
[2] *Faculty of Pharmacy, Osaka Ohtani University, Osaka, Japan.*

Summary **Phosphorothioate modification is one of the most widely investigated and promising chemical modifications in oligonucleotide (ON) based therapeutics. Structurally similar 5'-thio or phosphorothiolate-modified nucleotides, in which a 5'-bridging oxygen is replaced with a sulfur atom, are gaining importance for ON-based research. Several reports have been published describing the synthesis of 5'-thio-modified ONs but no detailed *in vitro* and *in vivo* data are available. Here, we report the synthesis of 5'-thio-modified 2'-deoxy-5-methylcytidine. 5'-Thio-modified thymidine and 2'-deoxy-5-methylcytidine were incorporated into target ONs, then we evaluated their binding affinity, nuclease stability, RNase H mediated scission, stability in blood serum, and *in vitro* and *in vivo* activity. This is the first report showing the influence of 5'-thio-modified antisense ONs in *in vitro* and *in vivo* experiments.**

Keywords: Phosphorothiolate, methylcytosine, RNase H activity, *in vitro* and *in vivo* antisense activity

1. Introduction

Nucleic acid analogues are widely used in biochemical research and oligonucleotide (ON) based therapy. The phosphorothioate modification (Figure 1A), in which a non-bridging oxygen covalently bound to phosphorus is replaced by a sulfur atom, is of considerable interest in ON-based therapy because of its ease of synthesis and the improved pharmacological properties of the modified ONs (*1-3*). However, these modified ONs contain chiral center at the phosphorus atom, resulting two stereoisomers referred to as Sp and Rp. Those stereoisomers have distinct physical and biochemical properties (*4,5*), and are very difficult to purify.

The 5'-thio modification (or phosphorothiolate modification) is structurally similar to the phosphorothioate modification, with a sulfur atom replacing the 5'-bridged oxygen connected to the ribofuranose sugar moiety (Figure 1B). The 5'-thio modification provides important biochemical probes for investigating fundamental features of enzyme catalysis and is a potential candidate for therapeutic applications (*6*). In addition, phosphorothiolates affect the ON sugar conformation, making them ideal for fine-tuning the potency of antisense DNA and small interfering RNAs (siRNAs). Furthermore, unlike phosphorothioates, phosphorothiolates do not have a chiral center at the phosphorous atom (*7,8*). The importance of the 5'-thio modification is reflected in the large number of synthetic chemical and enzymatic approaches reported to date, yet significant synthetic challenges remain for the fully automated solid-phase synthesis of 5'-thio phosphorothiolates (*9,10*). Recently Hofmann and Engels described a very convenient method for the synthesis of 5'-thio-modified ONs using an automated solid support DNA synthesizer (*11*). However, to our knowledge, despite the large body of work conducted on the chemical synthesis of 5'-thio-modified ONs such as a report describing ribozyme catalytic action on the phosphorothiolate linkage (*9*), there are no comprehensive studies on the *in vitro* and *in vivo* properties of 5'-thio-modified ONs yet. Given the potential of the 5'-thio modification to improve pharmacokinetic and pharmacodynamic properties, there is considerable interest in identifying new ON analogs exhibiting high *in vivo* efficacy and low toxicity (*12*). Here we describe the synthesis of ONs containing a 5'-thio-modified monomer using a fully automated

*These authors contributed equally to this works.
***Address correspondence to:*
Dr. Satoshi Obika, Graduate School of Pharmaceutical Sciences, Osaka University, 1-6 Yamadaoka, Suita, Osaka 565-0871, Japan.
E-mail: obika@phs.osaka-u.ac.jp

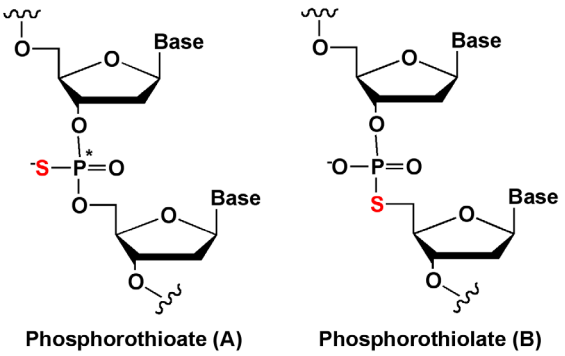

Figure 1. Chemical structure of a phosphorothioate (A) and a phosphorothiolate (B) linkage. *Chiral center.

solid support DNA synthesizer, as well as evaluation of their hybridizing ability with complementary strands, nuclease resistance, *in vitro* and *in vivo* bioassay, ribonuclease H (RNase H) mediated scission properties, and stability in blood serum.

2. Materials and Methods

2.1. *Materials*

All starting materials and reactants were purchased and used without further purification. Moisture-sensitive reactions were conducted in dried glassware under argon gas. All NMR spectrums were measured using JEOL-JNM (JEOL Resonance Inc., Tokyo, Japan) instruments. ^{1}H-NMR spectra were recorded at 300, 400 and 500 MHz. ^{13}C-NMR spectra were recorded at 75 and 100 MHz. ^{31}P-spectra were recorded at 202 MHz. IR spectrum and optical rotation data for all new compounds were measured using FT/IR-4200 (JASCO Corporation, Tokyo, Japan) and P-2200 (JASCO Corporation) respectively. Silica gel PSQ 60B (Fuji Silysia Chemical Ltd., Kasugai, Japan) was used for column chromatography. The progress of the reactions was monitored by analytical thin layer chromatography (TLC) on pre-coated aluminum sheets (Silica gel 60 F254-sheet, Merck KGaA, Darmstadt, Germany), and the products were visualized under UV light.

2.2. *Oligonucleotide synthesis*

ONs containing 5'-thio monomers were synthesized on an automated DNA synthesizer (ns-8, GeneDesign Inc., Ibaraki, Japan) using a conventional phosphoramidite method. 1.0 M *tert*-Butyl hydroperoxide in acetonitrile (Sigma-Aldrich Co. LLC, St. Louis, US) was used as an oxidizer instead of commonly used iodine. 5'-thio amidite monomers were successfully coupled using an extended coupling (8 min), detritrylation (26.5 min) and oxidation (5 min) times for the modified positions. The synthesized ONs were purified by reverse-phase HPLC (RP-HPLC, Shimadzu Inc., Kyoto, Japan) with Xbridge™ OST C18 column 2.5 µm (4.6 × 50 mm) (Waters Corporation, Milford, US) using 0.1M TEAA (triethylammonium acetate) buffer (pH 7.0) containing 50% MeCN (gradient: 5-17.5% MeCN over 20 min). Composition and purity were characterized by MALDI-TOF mass spectrometry (Autoflex II TOF/TOF mass spectrometer, Bruker Daltonics K.K., Yokohama, Japan) and RP-HPLC. Complementary RNA, DNA, and antisense oligonucleotides (ASOs) incorporated with 5'-thio-modified thymidine and 2'-deoxy-5-methylcytidine were synthesized by GeneDesign, Inc.

2.3. T_m *measurements*

UV melting experiments (*13*) were conducted using a SHIMADZU UV-1800 spectrometer (Shimadzu Inc., Kyoto, Japan) equipped with a T_m analysis accessory. The UV melting profiles were recorded by dissolving the oligonucleotide at 4 µM in 10 mM sodium phosphate buffer (pH 7.2) containing 100 mM NaCl, then scanning at 0.5°C/min and detecting at 260 nm. The temperature at which half the duplex dissociated was considered the T_m. The final T_m values were determined by averaging three independent measurements.

2.4. *Exonuclease stability assay*

Nuclease degradation experiments (*13*) were conducted by hydrolyzing ONs (750 pmol) at 37°C in buffer (100 µL) containing 50 mM Tris-HCl (pH 8.0), 10 mM $MgCl_2$, and 1 µg/mL phosphodiesterase I (GE Healthcare UK Ltd., Buckinghamshire, UK). Aliquots were removed at timed intervals (0, 2.5, 10, 20 and 40 min) and heated to 90°C for more than 2 min to deactivate the nuclease. The collected samples were analyzed by RP-HPLC (6-13% MeCN over 15 min) to evaluate the amount of intact ONs remaining (Figure S22, *http://ddtjournal.com/docindex.php?year=2016&kanno=5*). The percentage of intact ON in each sample was calculated and plotted against the digestion time to obtain a degradation curve.

2.5. *In vitro assay*

NMuLi cells (ATCC®, Manassas, VA), a cell line derived from mouse liver epithelium, were seeded at 3 × 10^3 cells/well in a 96-well plate and incubated in Dulbecco's Modified Eagle's Medium (DMEM, Nakalai Tesque, Kyoto, Japan) containing 10% heat-inactivated fetal bovine serum (FBS) without antibiotics in a 5% CO_2 incubator for 24 h. ASOs were transfected into cells using Lipofectamine 3000 (Thermo Fisher Scientific, Waltham, MA) without changing the medium according to the manufacturer's protocol. After 24 h, the cells were washed with phosphate buffered saline (PBS) once, then cell lysates were produced using the Lysis reagent in a SuperPrep® kit (TOYOBO, Osaka, Japan).

Reverse transcription (RT) was performed using the RT reagent in a SuperPrep® kit (TOYOBO) according to the manufacturer's procedure. The resulting cDNA template was used for quantitative PCR (qPCR) using TaqMan® Fast Universal PCR Master Mix (Thermo Fisher Scientific) and TaqMan® probe targeting phosphatase and tensin homolog (*Pten*) gene (Mm00477208_m1, Thermo Fisher Scientific) or *Gapdh* gene (Mm03302249_g1, Thermo Fisher Scientific). The expression level of each target gene was quantified using the ΔΔCt method, and the level of *Pten* mRNA was normalized to that of *Gapdh* mRNA. IC_{50} of each ASO was calculated by a sigmoidal curve fitting using Igor Pro software.

2.6. *In vivo assay*

All animal experiments were approved by the Institutional Animal Care and Use Committee of Osaka University. 7-week-old male C57BL/6J mice were obtained from Clea Japan (Tokyo, Japan) and were maintained on a 12-h light/12-h dark cycle and fed *ad libitum*. ASOs were intraperitoneally (*i.p.*) administered into individual mouse at 35 mg/kg (n = 4). After 72 h, all mice were sacrificed after anesthetization with isoflurane, perfused with PBS, and the livers were harvested, snap frozen, and the total RNA was isolated using a QuickGene RNA tissue kit SII (Wako, Tokyo, Japan) according to the manufacturer's protocol. Total RNA (1 μg) was reverse transcribed using a High Capacity cDNA Reverse Transcription kit (Thermo Fisher Scientific), then qPCR was performed as described above. Relative expression levels of *Pten* mRNA were evaluated against those of *Gapdh* mRNA. Aspartate aminotransferase (AST) and alanine aminotransferase (ALT) levels were analyzed in blood serum separated using a Microtainer brand tubes (#365967, Becton Dickinson, Franklin Lakes, NJ) from blood collected from the postcaval vein. AST and ALT levels in the blood serum were examined using a FUJI DRI-CHEM7000 clinical chemistry analyzer (Fujifilm, Tokyo, Japan) and FUJI DRI-CHEM slides: GOT/AST-PIII and GPT/ALT-PIII (Fujifilm).

2.7. *RNase H Digestion assay* (*13*)

5'-Cy3-labeled complementary RNA (0.5 μM) and individual antisense ONs (10 μM) were pre-mixed in 55 μL reaction buffer containing 40 mM Tris-HCl (pH 7.2), 150 mM NaCl, 4 mM $MgCl_2$, and 1 mM dithiothreitol (DTT). After incubation for 10 min at 37°C, 0.01 U/μL of *Escherichia coli* RNase H (Takara Bio Inc., Kusatsu, Japan) was added and the mixture was incubated at 37°C. Aliquots were removed at timed intervals and the reaction was terminated by mixing the aliquot with stop solution containing 35 mM EDTA and 2.5 M urea, followed by heating at 95°C for 5 min. The reaction samples were analyzed on 25% denaturing polyacrylamide gels containing 7 M urea, and 5'-Cy3-labeled RNA and digested products were visualized using Image Quant (LAS 4010, GE Healthcare) with a 20 s exposure time.

2.8. *Serum stability assay*

5'-Cy3-labeled ASOs were added to the serum separated from the 8-week-old C57BL/6J mouse blood as described in *in vivo* experiment procedure and the mixtures were incubated at 37°C. Aliquots were removed at timed intervals and the reaction was terminated at 95°C, then the 5'-Cy3-labeled ASOs and digested products were analyzed on 25% denaturing polyacrylamide gels containing 7 M urea. 5'-Cy3-labeled ASOs and digested products were visualized using Image Quant with a 20 s exposure time.

2.9. *Statistical analysis*

Pharmacological studies were performed using 4 mice per treatment group. All data are expressed as means ± S.D. $p < 0.01$ was considered to be statistically significant in all cases. Statistical comparisons of results were performed by Student's multiple comparison *t*-tests.

3. Results and Discussion

3.1. *Phosphoramidite monomer synthesis*

The 5'-thio thymidine phosphoramidite monomer **2a** was obtained as a previously described report (*11*). Then, from known nucleoside **2**, we synthesized the 2',5'-dideoxy-5'-thio-5-methylcytidine amidite monomer **5** (Scheme 1). Briefly, compound **2** was treated with acetic anhydride to obtain 3'-*O*-acetyl protected compound **3** in 84% yield. Benzyl protected 2'-deoxy-5-methylcytidine derivative **4** was obtained from compound **3** using known procedures (*14*) in 56% yield over three steps. Subsequent 3'-*O*-phosphitylation of **4** with 2-cyanoethyl-*N,N,N',N'*-tetraisopropylphosphorodiamidite provided the respective desired phosphoramidites **5** in 79% yield.

3.2. *T_m measurements*

The effect of the 5'-thio modification on duplex forming ability was estimated by measuring the melting temperature of the duplexes between **ON-2-5** and complementary DNA (cDNA) or RNA (cRNA) strands and comparing with those of the corresponding unmodified duplexes with **ON-1**/cDNA or **ON-1**/cRNA as described in Table 1. Single or multiple incorporation of the 5'-thio-modified monomer into different positions of the ONs showed acceptable differences in binding affinity following annealing to cDNA and cRNA (−2 to 1°C/modification).

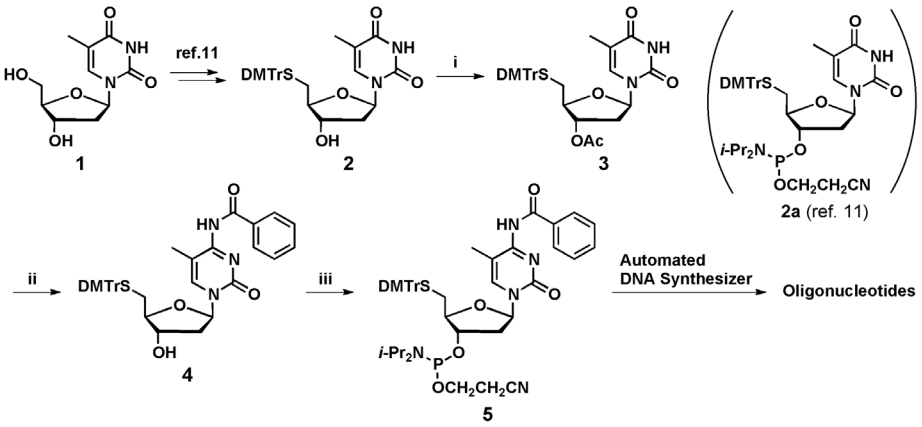

Scheme 1. Reagents and conditions. i. Ac_2O, pyridine, rt, 84%; ii. a. 1,2,4-triazole, $POCl_3$, TEA, MeCN, 0 °C to rt; b. Aq. NH_3, 1,4-dioxane, rt; c. benzoic anhydride, DMF, rt, 56% over 3 steps; iii. diisopropylammonium tetrazolide, 2-cyanoethyl-*N,N,N′,N′*-tetraisopropylphosphorodiamidite, MeCN, THF, rt, 79%.

Table 1. The sequences of 5'-thio modified oligonucleotides using T_m analysis or exonuclease resistance

Abbreviation	Sequences[b]	T_m (ΔT_m/modification) °C[a]	
		DNA[b]	RNA[b]
ON-1	5'-gcgtttttttgct-3'	50	45
ON-2	5'-gcgttt^{S}tttgct-3'	48 (-2.0)	45 (±0)
ON-3	5'-gcgtt^{S}t^{S}t^{S}ttgct-3'	44 (-2.0)	42 (-1)
ON-4	5'-gcgt^{S}tt^{S}tt^{S}tgct-3'	46 (-1.3)	43 (-0.7)
ON-5	5'-gcgttttttg^{Sm}ct-3'	50 (±0)	46 (+1)
ON-6	5'-ttttttttt-3'	N.D.	
ON-7	5'-ttttttttt$_{S}$t-3'	N.D.	
ON-8	5'-ttttttttt^{S}t-3'	N.D.	
ON-9	5'-ttttttttt^{m}c-3'	N.D.	
ON-10	5'-ttttttttt^{Sm}c-3'	N.D.	

ND: Not determined.
[a] UV melting profiles measured in 10 mM phosphate buffer (pH 7.2) containing 100 mM NaCl at a scan rate of 0.5°C/min at 260 nm.
[b] The concentration of oligonucleotide used was 4 μM for each strand. The sequence of complementary DNA or RNA is 5'-AGCAAAAAACGC-3'.
The black case represents natural DNA, and the red case represents as follows: ^{S}t, 5'-thio-t; ^{Sm}c, 5'-thio-^{m}c. The inferior case $_{S}$ indicates a phosphorothioate linkage.

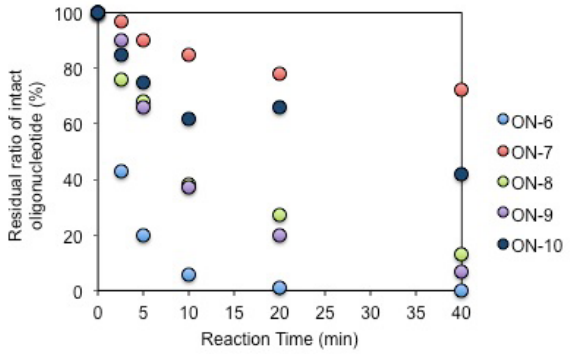

Figure 2. The ability of exonuclease resistance. Hydrolysis of ONs (750 pmol) conducted at 37°C in buffer (100 μL) containing 50 mM Tris-HCl (pH 8.0), 10 mM $MgCl_2$, and phosphodiesterase I (1.0 μg/mL). Sequences: 5′-d(TTTTTTTTTT)-3'; T = thymidine (light blue, **ON-6**), Phosphorothioate thymidine (red, **ON-7**), 5'-thio-thymidine (green, **ON-8**), 2'-deoxy-5-methycytidine (purple, **ON-9**), 2',5'-dideoxy-5'-thio-5-methycytidine (deep blue, **ON-10**).

3.3. *Exonuclease stability assay*

The enzymatic stability of the modified ONs was evaluated using phosphodiesterase I. Comparisons of the exonuclease stabilities of a series of oligonucleotides (**ON-6-10**) are shown in Figure 2. Under the conditions used in this experiment, oligonucleotide containing 2'-deoxy-5-methycytidine (**ON-9**) was more stable than oligonucleotide containing thymidine (**ON-6**). As expected, 5'-thio-modified oligonucleotides **ON-8** and **ON-10** had higher nuclease resistance compared to **ON-6** and **ON-9**, respectively. In contrast, phosphorothioate-modified oligonucleotide (**ON-7**) exhibited more enhanced stability against 3′-exonuclease compared to **ON-6** and **ON-9**.

3.4. *Design of antisense oligonucleotides for in vitro and in vivo assay*

We designed phosphorothioate antisense oligonucleotides (**ASO-1**, Table 2) targeting mouse *Pten* mRNA (NCBI ref: NM_008960.2), an LNA-DNA-LNA (2-8-2) gapmer containing a toxif motif (tgc) in the gap region (*15*). Gapmer design of two LNAs in each wing side with a ten natural nucleotide gap is believed to be sufficient to activate RNase H mediated cleavage of the target mRNA (*16*). Additionally, we prepared other antisense containing a 5'-thio-modified nucleoside, designated **ASO-2-4** as described in Table 2. Except for the 5'-thio modification sites, all those ASOs had a phosphorothioate backbone. In **ASO-2**, the 5'-thio modification was incorporated at the fourth and eighth positions from the 5'-end, whereas in **ASO-3** and **ASO-4**, a single 5'-thio modification was incorporated at the fourth or eighth position from the 5'-end, respectively. The potencies and toxicity characteristics of **ASO-2**, **ASO-3** and **ASO-4** were compared with the positive

Table 2. T_m values of 5'-thio modified oligonucleotides with complementary RNA[a]

Abbreviation	Sequences[b]	T_m (°C)[a]	IC_{50} (nM)[c]
ASO-1	5'-$T_s{}^mC_sa_st_sg_sg_sc_st_sg_sc_sa_sg_s{}^mC_sT$-3'	63.0	9.11
ASO-2	5'-$T_s{}^mC_sa_o{}^{St}t_sg_sg_sc_o{}^{St}t_sg_sc_sa_sg_s{}^mC_sT$-3'	61.5	15.3
ASO-3	5'-$T_s{}^mC_sa_o{}^{St}t_sg_sg_sc_st_sg_sc_sa_sg_s{}^mC_sT$-3'	61.0	6.99
ASO-4	5'-$T_s{}^mC_sa_st_sg_sg_sc_o{}^{St}t_sg_sc_sa_sg_s{}^mC_sT$-3'	61.1	32.2
ASO-5	5'-Cy3$_sT_s{}^mC_sa_st_sg_sg_sc_st_sg_sc_sa_sg_s{}^mC_sT$-3'	N.D.	N.D.
ASO-6	5'-Cy3$_sT_s{}^mC_sa_o{}^{St}t_sg_sg_sc_o{}^{St}t_sg_sc_sa_sg_s{}^mC_sT$-3'	N.D.	N.D.

ND: Not determined.
[a] UV melting profiles measured in 10 mM phosphate buffer (pH 7.2) containing 100 mM NaCl at a scan rate of 0.5°C/min at 260 nm.
[b] The concentration of oligonucleotide was 2 μM for each strand. The sequence of complementary RNA is 5'-AGCUGCAGCCAUGA-3'.
The black lower or upper case represents natural DNA or LNA, and the red case represents as follows: Stt, 5'-thio-t. The inferior case $_S$ or $_O$ indicates a phosphorothioate or a phosphodiester linkage, respectively.
[c] Each ASO was transfected into NMuLi cells using a lipofection method at the concentration of 0.25-200 nM.

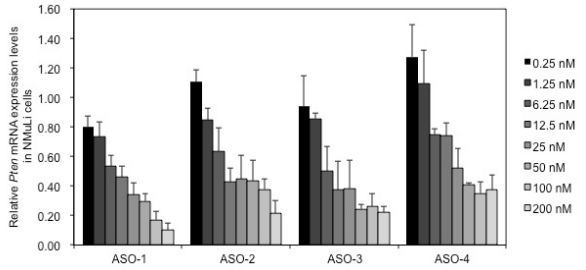

Figure 3. *In vitro* antisense efficiency of ASO-1, -2, -3, and ASO-4. Each ASO was transfected into NMuLi cells at the concentration of 0.25 nM to 200 nM using Lipofectamine3000. After 24 h, the cells were retrieved and the relative expression levels of *Pten* mRNA were determined.

control ASO-1. A thermal melting study was carried out and the T_m values of the ASOs with complementary RNA were determined. As expected, the affinity of all 5'-thio-modified ASOs (**ASO-2-4**) was essentially identical to that of **ASO-1** (Table 2).

3.5. *In vitro assay*

We evaluated the *in vitro* gene silencing properties of the ASOs in mice hepatic NMuLi cells (Figure 3) treated with 0.25-200 nM of each **ASO** in Table 2 using a lipofection method. A dose-dependent reduction of the *Pten* mRNA expression level was observed using qRT-PCR. Furthermore, 5'-thio-modified ASO at the fourth position from the 5'-end (**ASO-3**) showed very good *in vitro* gene silencing activity (Figure 3) with a high IC_{50} (7 nM). In contrast, 5'-thio-modified ASO at the fourth and eighth positions (**ASO-2**) or at the eighth position (**ASO-4**) had a low IC_{50} (13 nM or 28 nM), while the control **ASO-1** showed IC_{50} value of 9 nM.

3.6. *In vivo assay*

The *in vitro* results inspired us to evaluate the mRNA silencing activity of 5'-thio-modified ASO in an *in vivo* model. LNA-modified **ASO-1** (positive control) or 5'-thio-modified ASOs (**ASO-2**, **ASO-3**) were single-dose administered (*i.p.*) to 8-week-old male C57BL/6J mice at 35 mg/kg. After 72 h, all mice were sacrificed and the expression levels of *Pten* mRNA in the liver were analyzed. Figure 4A shows that the antisense oligonucleotide with a 5'-thio modification at the fourth and eighth positions from the 5'-end (**ASO-2**) exhibited almost no antisense activity and no reduction of mRNA expression, similar to that of the saline administered group, whereas LNA-modified **ASO-1** reduced the mRNA expression level by over 60%. On the other hand, **ASO-1** exhibited higher hepatotoxicity compared to **ASO-2** (Figure 4B). A single 5'-thio modification at the fourth position from the 5'-end (**ASO-3**) resulted in somewhat improved antisense activity (Figure 4C) but similar hepatotoxicity to that of **ASO-1** (Figure 4D). An ideal antisense oligonucleotide should exhibit high antisense activity with very low toxicity. These *in vivo* data showed that increasing the number of 5'-thio modifications reduced hepatotoxicity but unexpectedly reduced antisense activity as well.

3.7. *RNase H digestion assay*

RNase H activity provides important information for understanding the mechanism underlying the *in vivo* activity of ASOs. As described above, the *in vivo* activity was not as expected from the *in vitro* data and thus we conducted an RNase H mediated scission assay. Heteroduplexes of complementary RNA with the positive control gapmer antisense oligonucleotide (**ASO-1**) or with the 5'-thio-modified gapmer antisense oligonucleotide (**ASO-2-4**) were examined in the presence of RNase H (Figure 5). The degradation levels of 5'-Cy3-labeled complementary RNA (Cy3-RNA) in the heteroduplexes were analyzed as described above using denaturing-PAGE (Figure 5A). The residual ratios of Cy3-RNA were quantitated by calibrating the fluorescence intensity of Cy3-RNA, and the data were plotted against RNase H digestion time as shown in Figure 5B. The cleavage activity of each ASO against the Cy3-RNA is represented as the half-life ($t_{1/2}$) and the data are summarized in Figure 5C. Compared with **ASO-1**/RNA heteroduplex degradation activity ($t_{1/2}$ = 4.5 min), 5'-thio-modified ASOs more slowly

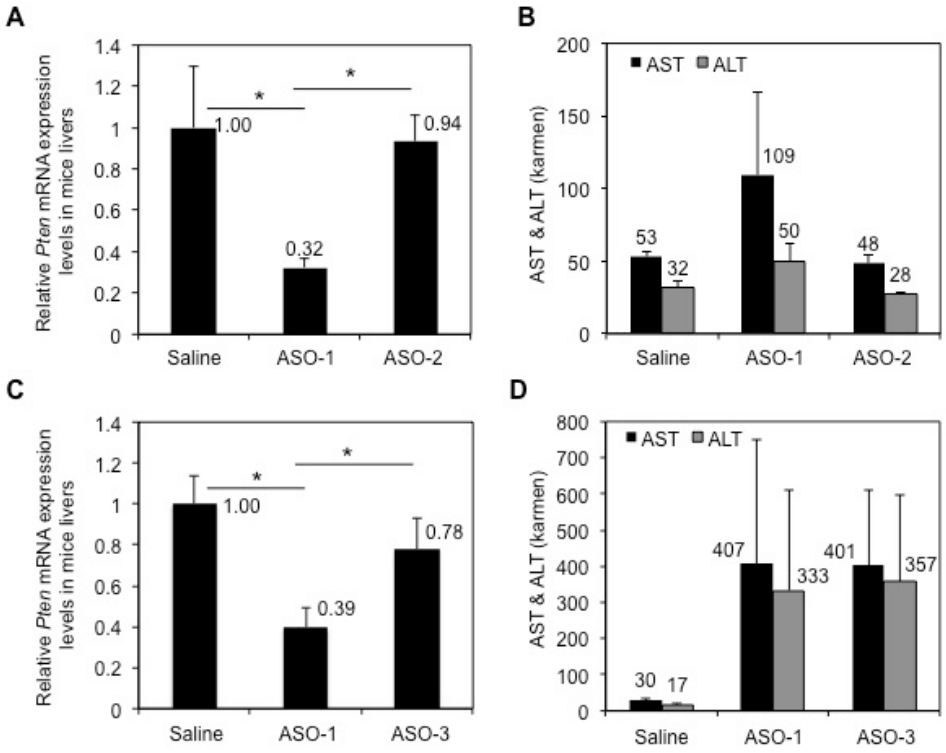

Figure 4. ***In vivo*** **antisense efficiency of ASO-1, -2, -3, and ASO-4 in mice liver.** Each ASO was intraperitoneally administered at 35 mg/kg. Mice were sacrificed after 72 h, and then, the relative expression levels of *Pten* mRNA in livers **(A**, **C)** and the AST, ALT levels in serum were calculated **(B**, **D)**. **p* < 0.01.

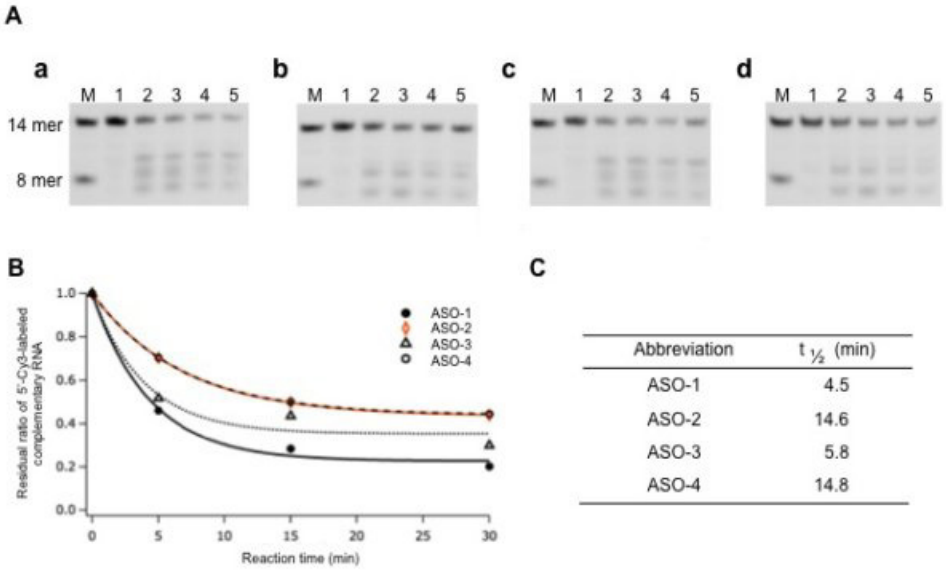

Figure 5. ***E. coli*** **RNase H activity analysis of ASO-1, -2, -3, and ASO-4. (A)** Denaturing PAGE analysis of 5'-Cy3-labeled complementary RNA forming duplexes with **ASO-1 (a)**, **ASO-2 (b)**, **ASO-3 (c)**, or **ASO-4 (d)** after *E. coli* RNase H reaction. M indicates the marker of 5'-Cy3-labeled of 14-mer RNA (5'-Cy3-AGCUGCAGCCAUGA-3') and 8-mer RNA (5'-Cy3-AGCUGCAG-3'). Lines 1-5 represent digestion time at 0, 5, 15, 30, and 60 min, respectively. Conditions of cleavage reaction: 5'-Cy3-labeled RNA (0.5 μM) and 19-22 (10 μM) in reaction buffer containing 40 mM Tris-HCl (pH 7.2), 150 mM NaCl, 4 mM $MgCl_2$, and 1 mM DTT at 37°C with 0.01 U/μL of *E. coli* RNase H. **(B)** Residual ratio of 5'-Cy3-labeled complementary RNA plots after *E. coli* RNase H reaction. **(C)** The half-life periods of 5'-Cy3-labeled complementary RNA forming duplexes with each ASO after *E. coli* RNase H reaction.

but effectively activated RNase H mediated scission. More specifically, **ASO-3** had almost the same half-life ($t_{1/2}$ = 5.8 min) compared with the positive control **ASO-1**. However, the RNase H activity of 5'-thio-modified ASOs at the eighth position or the fourth and eighth position from the 5'-end (**ASO-2**, **ASO-4**) was approximately three times weaker than that of **ASO-3**, indicating that an increase in the number of 5'-thio modifications or changing their position in the sequence was significant for the RNase H activity.

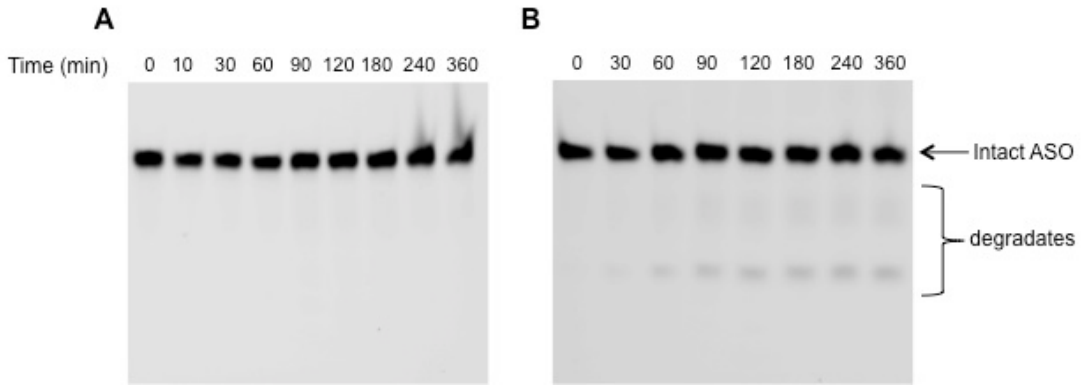

Figure 6. Serum stability assay of ASO-5 and ASO-6 in mouse blood serum. Denaturing PAGE analysis of 5'-Cy3-labeled ASO-1 **(ASO-5**, **A)** and **ASO-2 (ASO-6**, **B)** after adding to mouse serum at 37°C. The serum stability assay was examined up to 360 min.

The RNase H cleavage cascade has been previously reported as follows. First, RNase H binds to the 5' site of the target RNA, forming heteroduplexes with a gap region at the 3' site of the ASO (*17*). Next, the binding domain of RNase H recognizes the phosphorodiester or phosphorothioate linkages of the ASO at the 3' site of the gap region, then the catalytic domain of RNase H interacts with the target RNA at the gap region of the ASO (*17*). Gapmer ASO must contain successive 4-7 natural DNA nucleotides in gap region for the target RNA to be efficiently digested (*18,19*). Consequently, 5'-thio modification of the ASO at the fourth or at the fourth and eighth positions from the 5'-end site would influence RNase H digestion of the target RNA.

3.8. *Serum stability assay*

Chemically modified ASOs are generally more stable in blood serum than is natural DNA (*12*). However, our *in vivo* data suggested that the antisense activity of 5'-thio-modified ASOs may depend on the stability of the ASOs in serum. To confirm whether 5'-thio-modified ASO is stable in serum, we evaluated the blood serum stability of the ASO bearing the 5'-thio-modification at the fourth and eighth positions from the 5'-end (**ASO-2**) and compared it to LNA gapmer antisense oligonucleotide (**ASO-1**). 5'-Cy3 labeled **ASO-1** and **ASO-2** (**ASO-5**, **ASO-6**) was added to the serum collected from an 8-week-old C57BL/6J mouse and reacted for various lengths of time, then analyzed using denaturing-PAGE. As shown in Figure 6A, 5'-Cy3-labeled LNA gapmer ASO (**ASO-5**) was not degraded at all for 360 min. Fluorescently labeled 5'-thio-modified ASO (**ASO-6**) was essentially stable and little degradation was observed (Figure 6B). These results indicate that 5'-thio-modified ASO exhibits very good stability in blood serum and thus should reach the liver after ASO administration.

The *in vitro*, *in vivo*, RNase H activity and serum stability assay data showed discrepancies: the *in vitro* data showed that 5'-thio-modified ASO looked promising whereas the *in vivo* data did not. Initially, we thought that 5'-thio-modified ASO is not facilitated the RNase H mediated scission or is not stable at blood serum, but 5'-thio-modified ASO showed slow but significant RNase H activation as well as high stability in blood serum. Alternatively, it is possible that the sulfur atom at the 5' position alters pharmacokinetic properties such as protein binding and distribution, resulting in lower activity in the *in vivo* model.

4. Conclusion

In conclusion, we incorporated 5'-thio-modified derivatives into a series of ONs and evaluated their *in vitro* and *in vivo* biophysical properties. Inconsistencies between the *in vitro* and *in vivo* data remain unresolved and will be addressed in future studies.

Acknowledgements

One of us (Md Ariful Islam) would like to thank The Ministry of Education, Culture, Sports, Science and Technology (MEXT) of Japan for a research scholarship.

References

1. Matsukura M, Shinozuka K, Zon G, Mitsuya H, Reitz M, Cohen JS, Broder S. Phosphorothioate analogs of oligodeoxynucleotides: Inhibitors of replication and cytopathic effects of human immunodeficiency virus. Proc Natl Acad Sci U S A. 1987; 84:7706-7710.
2. Eckstein F. Nucleoside phosphorothioates. Annu Rev Biochem. 1985; 54:367-402.
3. Yamamoto T, Nakatani M, Narukawa K, Obika S. Antisense drug discovery and development. Future Med Chem. 2011; 3:339-365.
4. Oka N, Wada T. Stereocontrolled synthesis of oligonucleotide analogs containing chiral internucleotidic phosphorus atoms. Chem Soc Rev. 2011; 40:5829-5843.
5. Jahns H, Roos M, Imig J, Baumann F, Wang Y, Gilmour R, Hall J. Stereochemical bias introduced during RNA

synthesis modulates the activity of phosphorothioate siRNAs. Nat Commun. 2015; 6:6317.
6. Li NS, Tuttle N, Staley JP, Piccirilli JA. Synthesis and incorporation of the phosphoramidite derivative of 2′-*O*-photocaged 3′-*S*-thioguanosine into oligoribonucleotides: Substrate for probing the mechanism of RNA catalysis. J Org Chem. 2014; 79:3647-3652.
7. Li NS, Frederiksen JK, Piccirilli JA. Synthesis, properties, and applications of oligonucleotides containing an RNA dinucleotide phosphorothiolate linkage. Acc Chem Res. 2011; 44:1257-1269.
8. Gaynor JW, Cosstick R. Synthesis, properties and application of nucleic acids containing phosphorothiolate linkages. Curr Org Chem. 2008; 12:291-308.
9. Li NS, Tuttle N, Staley JP, Piccirilli JA. Synthesis and incorporation of the phosphoramidite derivative of 2′-O-photocaged 3′-S-thioguanosine into oligoribonucleotides: Substrate for probing the mechanism of RNA catalysis. J Org Chem. 2014; 79:3647-3652.
10. Connolly BA, Rider P. Chemical synthesis of oligonucleotides containing a free sulphydryl group and subsequent attachment of thiol specific probes. Nucleic Acids Res. 1985; 13:4485-4502.
11. Hofmann KJ, Engels JW. Efficient solid phase synthesis of cleavable oligodeoxynucleotides based on a novel strategy for the synthesis of 5'-S-(4,4'-dimethoxytrityl)-2'-deoxy-5'-thionucleoside phosphoramidites. Helv Chim Acta. 2004; 87:2812-2828.
12. Wahlestedt C, Salmi P, Good L, *et al*. Potent and nontoxic antisense oligonucleotides containing locked nucleic acids. Proc Natl Acad Sci U S A. 2000; 97:5633-5638.
13. Mitsuoka Y, Fujimura Y, Waki R, Kugimiya A, Yamamoto T, Hari Y, Obika S. Sulfonamide-bridged nucleic acid: Synthesis, high RNA selective hybridization, and high nuclease resistance. Org Lett. 2014; 16:5640-5643.
14. Koshkin AA. Conformationally restricted triplex-forming oligonucleotides (TFOs) binding properties of α-L-LNA and introduction of the N^7-glycosylated LNA-guanosine. Tetrahedron. 2006; 62:5962-5972.
15. Burdick AD, Sciabola S, Mantena SR, Hollingshead BD, Stanton R, Warneke JA, Zeng M, Martsen E, Medvedev A, Makarov SS, Reed LA, Davis JW, Whiteley LO. Sequence motifs associated with hepatotoxicity of locked nucleic acid–modified antisense oligonucleotides. Nucleic Acids Res. 2014; 42:4882-4891.
16. Yamamoto T, Harada-Shiba M, Nakatani M, Wada S, Yasuhara H, Narukawa K, Sasaki K, Shibata MA, Torigoe H, Yamaoka T, Imanishi T, Obika S. Cholesterol-lowering action of BNA-based antisense oligonucleotides targeting PCSK9 in atherogenic diet-induced hypercholesterolemic mice. Mol Ther Nucleic Acids. 2012; 1:e22.
17. Lima WF, Rose JB, Nichols JG, Wu H, Migawa MT, Wyrzkiewicz TK, Siwkowski AM, Crooke ST. Human RNase H1 discriminates between subtle variations in the structure of the heteroduplex substrate. Mol Pharmacol. 2007; 71:83-91.
18. Kurreck J, Wyszko E, Clemens G, Erdmann V. Design of antisense oligonucleotides stabilized by locked nucleic acids. Nucleic Acids Res. 2002; 30:1911-1918.
19. Crooke ST, Lemonidis KM, Neilson L, Griffey R, Lesnik EA, Monia BP. Kinetic characteristics of *Escherichia coli* RNase H1: Cleavage of various antisense oligonucleotide-RNA duplexes. Biochem J. 1995; 312:599-608.

(Received August 30, 2016; Revised October 22, 2016; Accepted October 24, 2016)